Research Article

Yiyi Shi, Jianqiao Liu, Pengyu Yang, Hongzhen Wang*, Shanshan Guan, and Jiyuan Cui

Surface modification of sepiolite and its application in one-component silicone potting adhesive

https://doi.org/10.1515/epoly-2024-0051
received May 14, 2024; accepted August 2, 2024

Abstract: In this study, the utilization of sepiolite (SEP), renowned for its remarkable water absorption capacity, in a one-component silicone potting adhesive was explored to evaluate its impact on the efficacy of tunnel crack injection adhesive. Initially, SEP underwent high-temperature calcination, and X-ray diffraction and thermogravimetric tests were conducted to analyze the influence of calcination on its crystal structure and water-absorption capacity, respectively. Following this, various coupling agents were employed to modify the SEP, and their respective impacts on the performance of the tunnel crack-filling adhesive were investigated. The outcomes revealed that KH550 exhibited the most effective modification. Subsequent analysis delved into the effect of varying the dosage of KH550 on adhesive performance, demonstrating optimal cost-effectiveness at a dosage of 2 phr. Furthermore, a comparative assessment of the adhesive's performance in wet and dry interfaces revealed that the addition of SEP resulted in comparable bond strength between wet and dry interfaces, indicating minimal influence from the wet interface.

Keywords: surface modification, sepiolite, potting adhesive, water-absorption

1 Introduction

Leakage remains a prevalent issue in tunnel engineering, significantly compromising the durability of lining structures, particularly when faced with corrosive groundwater, exacerbating the ramifications. Grouting technology stands as a highly effective solution to mitigate such leakage disasters (1,2). However, the choice of grouting materials holds pivotal significance in successfully addressing these challenges. Several critical aspects factor into material selection: (1) the slurry's viscosity should be low, facilitating penetration into fissures. (2) Optimal gelling time is imperative to prevent premature slurry washout before full sealing. (3) Material stability, high compressive strength, and resistance to secondary hazards are essential regardless of environmental conditions and temperature variations. (4) Non-toxicity, harmlessness to the environment, especially to water sources, is fundamental. (5) Compatibility with grouting pipes and equipment to ensure efficient application. (6) Resistance to pressure and aging for sustained effectiveness. (7) Simplified selection, accessibility, and reasonable pricing contribute to practical application (3–5). One-component liquid silicone rubber (6,7), a viscous liquid, cures upon contact with trace moisture in the air at room temperature, forming a three-dimensional mesh structure resembling ordinary vulcanized rubber in physical and mechanical properties. Its characteristics encompass exceptional weather resistance, aging resistance, moisture resistance, shock resistance, high bond strength, unaffected curing by water, good elasticity, and controllable curing time, making it an ideal material for tunnel grouting. However, the challenge arises during application when the tunnel surface is wet or covered in a water film, significantly compromising the adhesive properties of the silicone rubber (8–11). Research by Quang Khieu et al. (12) elucidated that silane crosslinker molecules, upon exposure to water, transform into highly aqueous forms, hampering the crosslinking reaction of silicone rubber (13). Hence, seeking a water-absorbing filler to address moisture-related interface issues stands as a primary research direction in perfusion rubber.

* **Corresponding author: Hongzhen Wang**, School of Polymer Science and Engineering, Qingdao University of Science & Technology, 266042 Qingdao, China, e-mail: qustwhz@163.com
Yiyi Shi, **Jianqiao Liu**, **Shanshan Guan**, **Jiyuan Cui:** School of Polymer Science and Engineering, Qingdao University of Science & Technology, 266042 Qingdao, China
Pengyu Yang: CCCC Tunnel and Bridge (Nanjing) Technology Co., Ltd., Nanjing, 211899, China

Sepiolite (SEP), a fibrous magnesium-rich silicate clay mineral renowned for its strong water-absorbing properties, possesses a crystalline structure featuring alternating rows of silica-oxygen tetrahedra and magnesium-oxygen octahedra, creating a 2:1 layered structural unit with channels arranged parallel to the interlayers (14–18). Its unique structure comprises internal nano-pass-through pores, external grooves (19–21), and surface hydroxyl group-rich properties, stable even at high temperatures. Zhang et al.'s (22) investigation on SEP fibers' phase transition and morphology highlighted its water adsorption mechanisms – physisorption and chemisorption – attributed to tubular zeolite water channels, hydrophilic Si–OH groups, and Mg^{2+} ligand water (23). Theoretically, SEP can absorb 200% to 250% of its weight in water (24). Notably, the absorbed water undergoes strong surface chemisorption and capillary channel effects, making it less prone to desorption compared to hygroscopicity. Despite high water absorption, SEP does not expand significantly after uptake (25).

The primary goal of this study is to develop a one-component silicone rubber potting adhesive capable of retaining robust adhesive strength even in wet interfaces. To achieve this, SEP is utilized to prepare one-component silicone rubber, leveraging its water-absorbing properties to neutralize the impact of moisture on grouting glue, consequently enhancing adhesive strength and stability. This pioneering approach offers crucial theoretical and practical insights for future advancements in tunnel silicone rubber grouting materials.

2 Experimental materials and methods

2.1 Materials

Dayi Chemical Co., Ltd. (Yantai, Shandong, China) offers α,ω-dihydroxy polydimethylsiloxanes with viscosities of 20,000 and 1,000 cps and Qingdao Zhongxiang Environmental Protection Technology Co., Ltd. offers SEP. Hangzhou Guibao Chemical Co., Ltd. (Hangzhou, Zhejiang, China) offers methyltributylketone oxime silane (T30), vinyltributylketone oxime silane (T90), and dimethyldibutylketone oxime silane (3002). Sinopharm Chemical Reagent Co., Ltd. offers organotin catalyst (dibutyltin dilaurate), γ-aminopropyltriethoxysilane (KH550), vinyltrimethoxysilane (A171), γ-glycidyl ether oxidizedpropyltrimethoxysilane (KH560), lightweight calcium carbonate, calcium oxide, and chloroform.

2.2 Surface modification of SEP

Calcined SEP at 350°C for 2 h. The modifier was mixed into the calcined SEP under dry conditions. In a 500 mL glass reactor, 100 g of calcined SEP was mixed with corresponding portions of modifier (2 g A171, 2 g KH560, 2 g KH550, 1 g KH550, 3 g KH550) and 300 mL of chloroform, respectively. The reaction mixture was stirred with a magnetic stirrer at room temperature for 24 h. The mixture was then washed with 100 mL of chloroform and filtered with filter paper over a pressure funnel. It was then dried in an oven at 80°C for 24 h. The dried functionalized SEP was ground and then sieved through a sieve. The samples were named as follows: SEP-A171, SEP-KH560, SEP-KH550 (SEP-2KH550), SEP-1KH550, and SEP-3KH550. and the samples were analyzed by Fourier transform infrared (FTIR) spectrometry, thermogravimetric analysis (TGA) (thermal stability), and other means, respectively.

2.3 Experimental formulation and preparation of one-component silicone rubber potting adhesive

The experimental formulation of one-component silicone rubber is shown in Table 1.

The preparation of one-component silicone rubber is as follows. Different viscosities of α,ω-dihydroxy polydimethylsiloxane were first put into a double planetary mixer and stirred homogeneously, and then fillers such as SEP treated with a coupling agent were put in, and after stirring and mixing homogeneously, it was heated to 120°C and vacuumed for 0.5–1 h to further remove the water in the filler and volatile components in the rubber, and then, it stopped stirring and cooled down to room temperature. In the nitrogen atmosphere, were added to the crosslinking agent, chain extender, and catalyst, stirring uniformly to obtain a one-component room temperature curing liquid silicone rubber.

2.4 X-ray diffraction (XRD) analysis

The changes in the crystal structure and interlayer structure of SEP before and after calcination were analyzed using a Bruker AXS D8 Advance X-ray diffractometer from Germany. The X-ray tube was selected to be a Cu-Kα target, with a 30 mA working current, a 40 kV working voltage, and a diffraction angle of 2θ in the scanning range of 5–90°.

Table 1: The experimental formulation (g)

Raw materials	1	2	3	4	5	6	7	8	9
α,ω-Dihydroxypolydimethylsiloxane (20,000 cps)	90	90	90	90	90	90	90	90	90
α,ω-Dihydroxypolydimethylsiloxane (1,000 cps)	10	10	10	10	10	10	10	10	10
Calcium carbonate	40	40	40	40	40	40	70	40	40
Calcium oxide								30	15
SEP	30	30	30	30	30	30			15
A171		0.6							
KH550			0.6		0.3	0.9			0.15
KH560				0.6					
Vinyltributylketoxime silane (T90)	4	4	4	4	4	4	4	4	4
Methyltributylketoxime silane (T30)	4	4	4	4	4	4	4	4	4
Dimethyldibutanone oxime silane (3002)	4	4	4	4	4	4	4	4	4
Organotin catalysts (dibutyltin dilaurate)	0.1	0.1	0.1	0.1	0.1	0.1	0.1	0.1	0.1

2.5 Thermogravimetric analysis

TGA and DTG measurements were carried out using a TGA-7 thermal analyzer (PerkinElmer, USA) between 35 and 800°C at a ramping rate of 20°C·min^{-1}, with a protective atmosphere of nitrogen (N_2) atmosphere.

2.6 FTIR spectroscopy

Infrared spectroscopy (FTIR): FTIR spectra were recorded using a Bruker Tensor 27 spectrometer (Bruker, Germany), and the samples were characterized in infrared using the attenuated total reflection mode, with a scanning range of 600–4,000 cm^{-1}, a resolution of 4 cm^{-1}, and 32 scans for each sample.

2.7 Scanning electron microscope (SEM) analysis

The microscopic morphology of SEP before and after modification was observed by using a JSM-6700F (Nippon Electronics Corporation) microscope.

2.8 Tack free time

GB/T 13477. 5-2002 building sealing materials test method to determine the tack-free time of the adhesive mixture. In this work, the conditions for measuring the tack-free time are a temperature of 25°C and a humidity of 50%. The rubber material from the sealed package was placed at a temperature of 25°C and a humidity of 50% environment. Wipe the fingertips with anhydrous hexanol, gently touch different parts of the mixed adhesive surface, and repeat the above operation at appropriate intervals until no adhesive adheres to the fingers. Record the time from the removal of the adhesive from the sealed package to the adhesive mixture does not adhere to the finger, that is, the tack free time.

2.9 Viscosity testing

A Brookfield rotational viscometer was used to determine the viscosity of the infused adhesive using a No. 6 rotor at a speed of 25 rpm.

2.10 Mechanical properties

The tensile strength and elongation of silicone rubber are tested according to GB/T 528-2009. The tensile rate is 500 mm·min^{-1}.

2.11 Shear bonding performance

The shear bonding performance of the potting adhesive was tested in accordance with the GB/T13477.8-2017 standard.

3 Results and discussion

In this experimental setup, α,ω-dihydroxy polydimethylsiloxane served as the fundamental material. Calcium carbonate, SEP, and calcium oxide were chosen as fillers to create a one-component silicone rubber potting adhesive sealing material. This composite exhibited exceptional

resistance to interfacial moisture, weathering, impressive elasticity, impermeability, and superior bond strength.

3.1 XRD of SEP before and after calcination

One-component silicone rubber demands precise control over the filler's moisture content, and given SEP's inherent water-absorbing nature, preliminary dehydration of SEP becomes imperative. To achieve this, we subjected the SEP to a dehydration process by calcination at 350°C for 2 h, effectively eliminating its moisture content. To ensure the integrity of its crystal structure post-treatment, we conducted XRD analyses on both untreated SEP and SEP calcined at 350°C. The resulting XRD spectra of SEP, before and after calcination, are depicted in Figure 1.

Due to the intricate mineral composition and the presence of impurities within SEP, the XRD diagram reveals numerous diffraction peaks. Among these, the distinct diffraction peak at $2\theta = 7.3°$ signifies a characteristic feature of SEP. Notably, upon comparing the XRD patterns of SEP before and after calcination, it is evident that the majority of diffraction peaks remained unchanged. This consistency in peak positions suggests that the heat treatment applied to SEP within this temperature range did not alter its crystal structure.

3.2 Water absorption of SEP

To confirm the sustained water adsorption capacity of the calcined SEP, we subjected it to a 25°C environment with 100% humidity for 4 h after its calcination at 350°C. Subsequently, we

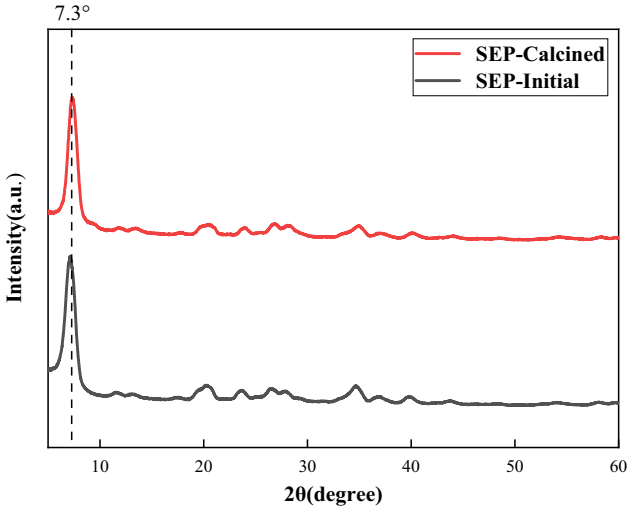

Figure 1: XRD spectra of SEP before and after calcination.

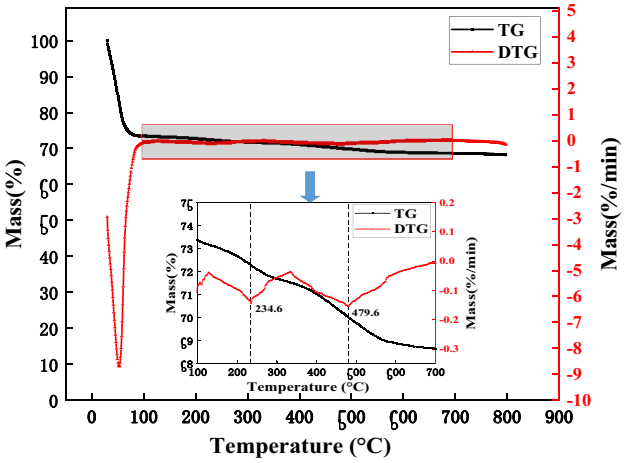

Figure 2: TG and DTG curves of SEP.

conducted a TGA. Figure 2 illustrates the thermogravimetric (TG) and DTG graphs. They demonstrated the relationship between the amount of sep substance and temperature at programmed temperature, and compared with TG curve, DTG curve can more directly reflect the dynamic change of SEP mass during heating process, which helps to analyze the thermal properties of samples more accurately. while Table 2 presents the data sheet detailing the analysis of water absorption by SEP.

The data reveal a triphasic release of water within SEP. The initial stage, occurring between 29.5°C and 127°C, predominantly comprises adsorbed water, constituting 26.7% of the total mass, representing the primary component of SEP's water content. Notably, the most rapid water volatilization occurs around 53.5°C during this phase. The subsequent stage spans 127–334°C and chiefly involves zeolite water, accounting for 2.7% of the total mass. Notably, the crystal structure of SEP remains intact during these first two stages, with water absorption primarily through physical adsorption, allowing for a reversible process of water absorption and dehydration. The final stage occurs in the range of 334–800°C, primarily attributed to the loss of weight due to crystalline water and structural water (22), constituting a moisture content of 0.6% of the total mass. This elucidates SEP's exceptional water absorption capabilities, underscoring its capacity to absorb water through distinct stages with varying water components.

3.3 Infrared spectra of modified SEP

Through functionalization modification using silane coupling agents, surface functional groups are introduced onto this natural silicate. These groups readily engage in

Table 2: TGA data of SEP

Sample	T_{max1} (°C)	Residues at the first stage (wt%)	T_{max2} (°C)	Residues at the second stage (wt%)	T_{max3} (°C)	Residues at the third stage (wt%)
SEP	54	73	235	71	480	70

Notes: T_{max1}, T_{max2}, T_{max3} – maximum decomposition temperature in the first, second, and third stages, respectively.

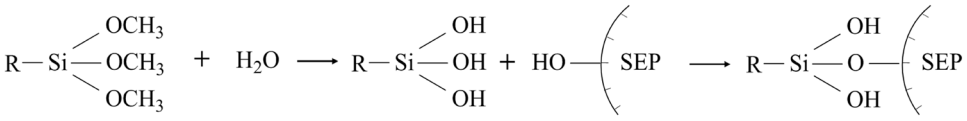

Figure 3: Schematic reaction of coupling agent modified SEP.

reactions with the resin, thereby augmenting the interfacial bond strength between the resin and SEP. This enhancement significantly contributes to improving the properties of the resultant silicone adhesives (26–30).

The grafting of SEP with coupling agents involves a two-step process. First, under specific conditions, the coupling agent undergoes hydrolysis, resulting in the formation of hydroxyl-containing silanols. Subsequently, a reaction occurs between these silanols and the active hydroxyl groups present on the surface of SEP, leading to dehydration and condensation reactions that generate Si–O–Si bonds. The schematic representation of this reaction between the coupling agent and the active hydroxyl groups on the SEP surface is depicted in Figure 3.

This study involved endeavors to modify SEP utilizing A171, KH550, and KH560, respectively. The modified SEP underwent characterization via infrared spectra analysis, and the results of these analyses are illustrated in Figure 4.

SEP exhibits distinctive features in its infrared spectrum, showcasing characteristic absorption peak positions such as OH stretching vibrations at 4,000–3,600 cm^{-1}, M-OH stretching vibrations at 3,400 cm^{-1}, and Si–O stretching vibrations at 1,070 cm^{-1}. Figure 4 displays the IR spectra of untreated SEP alongside SEP modified using A171, KH550, and KH560. The modified versions of SEP – A171-SEP, KH550-SEP, and KH560-SEP – reveal additional absorption peaks of $-CH_2$ at 2,920 and 2,850 cm^{-1}. This presence confirms the successful grafting of all three modifiers onto the surface of SEP.

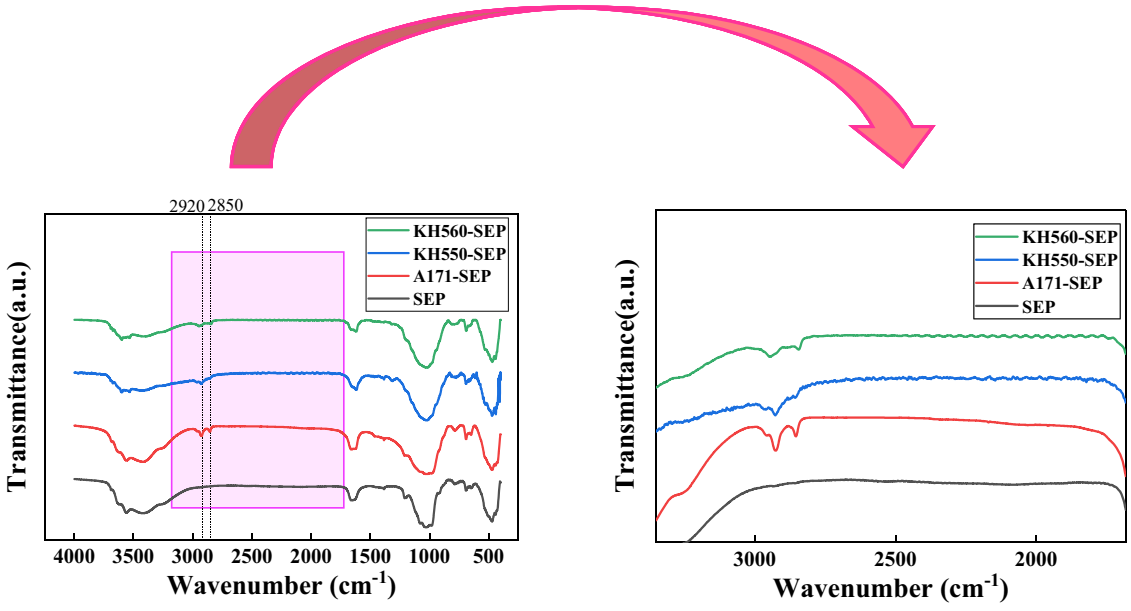

Figure 4: Infrared spectra of SEP before and after modification.

3.4 Effect of different modifiers modified SEP on the properties of one-component silica gel

The curing speed, fluidity, and mechanical attributes significantly influence the application of the perfusion adhesive. Tack-free time, a crucial metric, denotes the duration for the adhesive exposed to specific ambient conditions – temperature and relative humidity – after which its surface, when touched, exhibits vanished viscosity and non-stickiness. A shorter tack-free time implies a faster adhesive curing reaction. The viscosity of the adhesive profoundly impacts its construction parameters. Excessive viscosity hampers fluidity and perfusion performance, while inadequate viscosity compromises mechanical properties and prolongs surface drying. Achieving an appropriate viscosity is pivotal for optimal construction performance. Adhesive strength signifies the bond between the perfusion adhesive and the substrate, typically necessitating a strength greater than 1 MPa. Additionally, tensile strength and elongation at break constitute fundamental mechanical properties of the material. In perfusion adhesive applications, the desired criteria usually involve tensile strength surpassing 1.5 MPa and elongation at break exceeding 200%.

Figure 5 illustrates the impact of different modifiers on SEP properties concerning one-component silica gel. Observing Figure 5a, it is evident that SEP modified with KH550 and KH560 significantly reduced the tack-free time of the infused adhesive, whereas the modification with A171 resulted in a lengthened tack-free time, because the modifier affects the pH environment after hydrolysis, which affects the reaction rate of the crosslinker, resulting in a change in the tack-free time. Regarding Figure 5b, the modified SEP displayed notably decreased viscosity, with KH550-modified SEP exhibiting the lowest viscosity, because the compatibility between the modified SEP and silica gel has been improved to varying degrees, among which KH550 has the best compatibility with silica gel, so its viscosity is

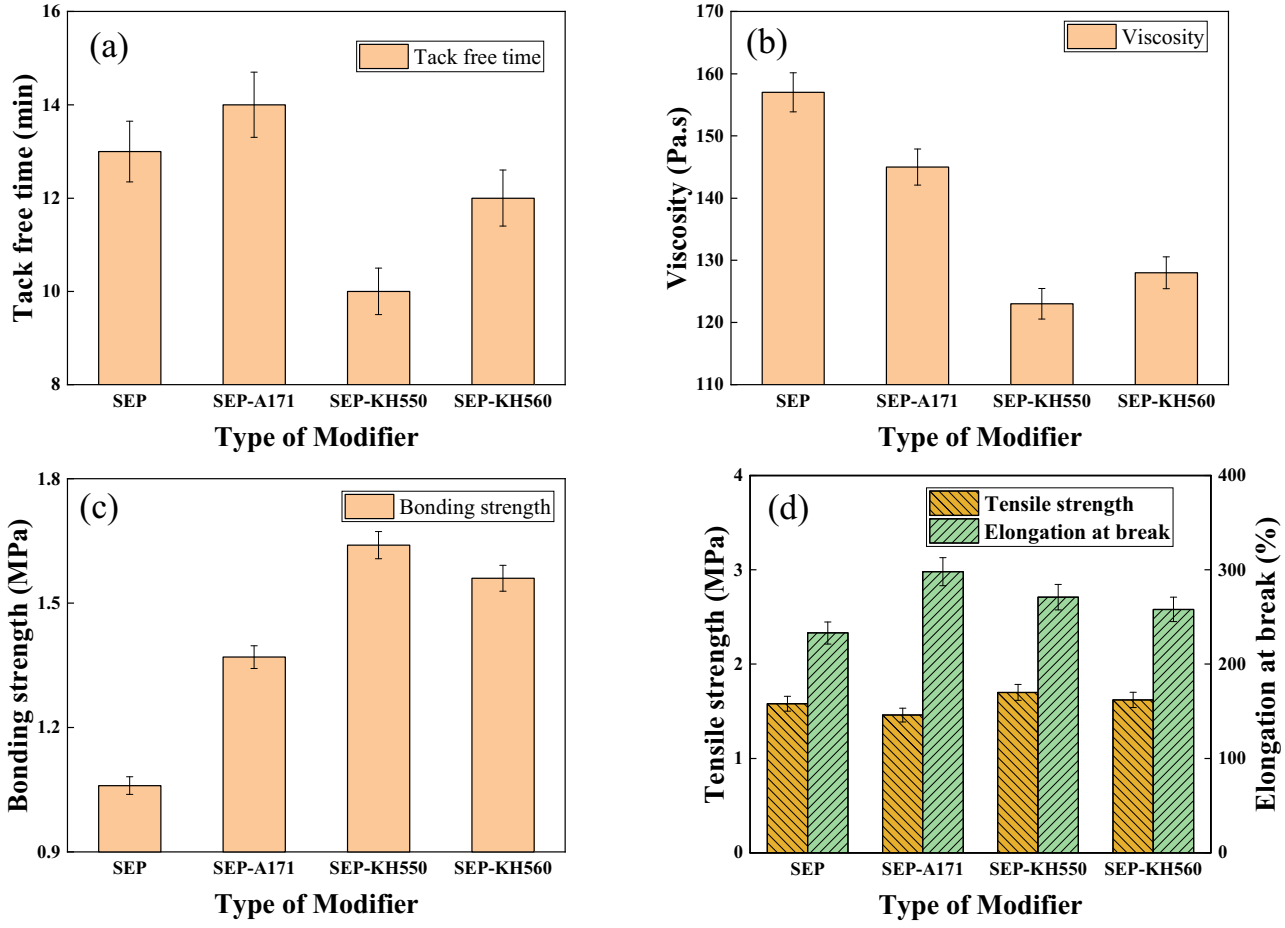

Figure 5: The effect of SEP modified with different modifiers on the properties. (a) Tack free time; (b) Viscosity; (c) Bonding strength and (d) Tensile strength) of one-component silica gel.

the lowest. Examining Figure 5c reveals an enhancement in adhesive strength post-SEP modification. Specifically, the adhesive strength was notably highest for the perfusion adhesive utilizing KH550-modified SEP, because the modifier contains a large number of active functional groups, which increases the interaction between the material and the matrix. KH550 is rich in $-NH_2$, which can form a large number of hydrogen bonds with the matrix so that the adhesive strength of the material is greatly improved. Figure 5d demonstrates an overall improvement in the elongation properties of the perfusion adhesives following SEP modification, with marginal changes observed in tensile strength. While the tensile strength marginally increased with KH550 and KH560 modified SEP, a slight decrease was observed with A171 modified SEP, because the dispersion of the modified SEP is improved, so that the elongation increases, and the tensile strength is enhanced, A171 is vinyl trimethoxysilane, which is also the crosslinking agent of the dealcoholized silicone glue, and its bond energy is slightly lower than that of the deketoxime silica gel, so the tensile strength is slightly reduced. In summary, the perfusion adhesive prepared using KH550-modified SEP exhibited the most favorable overall performance among the evaluated modifiers.

3.5 SEM electron micrographs

Figure 6 presents SEM images comparing unmodified SEP with KH550 modified SEP and their SEM images in the silicon rubber. The unmodified SEP exhibits a morphology of rod-shaped fiber aggregates, where the boundaries between fibers are indistinct, signifying more pronounced agglomeration. This agglomeration impedes the effective dispersion of SEP within the rubber matrix, potentially causing stress concentration and consequent reduction in mechanical properties. Contrastingly, the SEM images of modified SEP depict the dispersion of SEP in the form of individual fibers, with more distinct boundaries between them. The unmodified SEP was locally agglomerated in the silica gel, while the modified SEP was uniformly dispersed in the silica gel. This observation indicates that the modification with the coupling agent diminishes

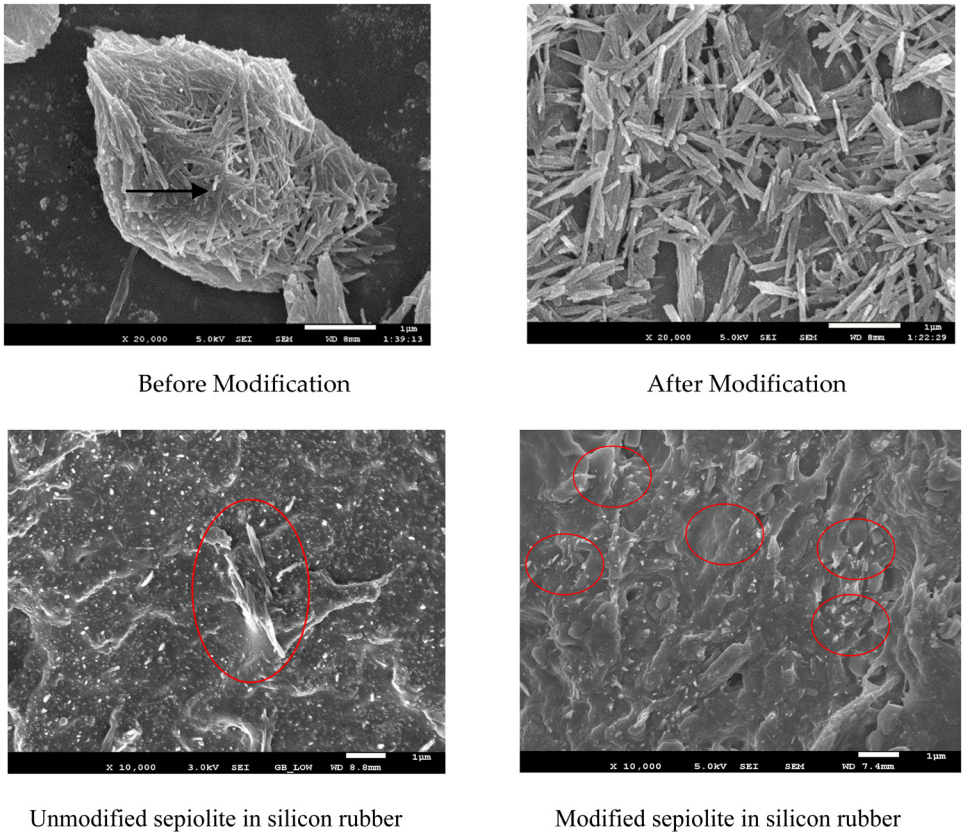

Figure 6: SEM photographs of SEP before and after modification (Scale bar = 1 μm).

the surface energy of SEP fibers, thereby reducing fiber agglomeration. This reduction is beneficial, as it enhances the dispersion of SEP fibers within the rubber matrix.

3.6 Effect of KH550 dosage on the properties of SEP

To obtain cost-effective formulations, this work further investigated the effect of the dosage of KH550 on the properties of SEP. The data are shown in Figure 7.

In Figure 7a, the reduction in the tack-free time of the perfusion adhesive correlates significantly with the escalating KH550 dosage. This outcome can be attributed to KH550's composition containing amino groups, alkaline in nature, which facilitate and accelerate the cross-linking agent's reaction rate (31). Figure 7b illustrates a noticeable decrease in the viscosity of the perfusion adhesive post-KH550 modification. However, as the KH550 dosage increases, the viscosity reduction gradually diminishes, plateauing when the dosage elevates from 2 to 3 phr. Because the compatibility between SEP modified by KH550 and silica gel has been greatly improved, so that the viscosity of the infusion glue is the lowest, and when the amount of KH550 is enough, the viscosity will not be reduced. Regarding adhesive strength, Figure 7c demonstrates a substantial enhancement post-KH550 modification; yet, the rate of increase declines with higher KH550 dosages. When the dosage reaches 3 phr, the adhesive strength shows only a 3.4% increase. Because the modifier KH550 contains a large number of amino groups, which can form a large number of hydrogen bonds with the matrix, improve the interaction force between the material and the matrix, so that the adhesive strength of the material is greatly improved, when the amount of KH550 is enough, the material mainly occurs is the body damage, and the size of the adhesive strength mainly depends on the strength of the material itself. Tensile strength and elongation, depicted in Figure 7d, exhibit significant improvements after KH550 modification. Nevertheless, the rate of tensile strength increase diminishes with escalating KH550 dosages – when increased from 2 to 3 phr, the tensile strength elevates by a mere 1.1%. Elongation initially rises with increasing KH550 dosage but then starts decreasing. Because the dispersion of SEP after KH550 modification increases, tensile strength and elongation increase, when the amount of KH550 increases to a certain extent, the dispersion of SEP can no longer continue to improve, and the tensile strength no longer changes

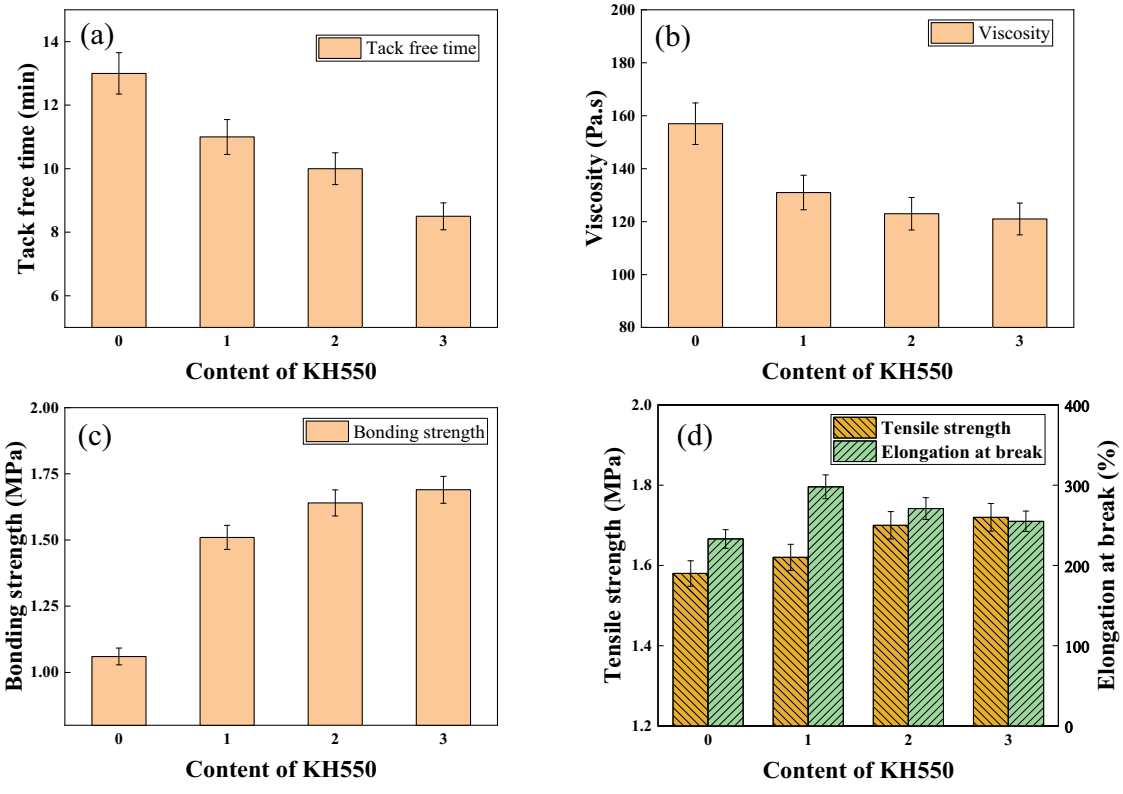

Figure 7: The effect of different KH550 dosage-modified SEP on the performance. (a) Tack free time; (b) Viscosity; (c) Bonding strength and (d) Tensile strength of one-component silica gel.

significantly, but the elongation shows a downward trend due to the enhancement of hydrogen bonding. In summary, the KH550-modified SEP remarkably enhances the overall performance of the perfusion adhesive. However, beyond a 2 phr dosage of KH550, the adhesive's performance improvements become negligible. Therefore, from both a performance and economic standpoint, a dosage of 2 phr for KH550 stands out as the optimal choice.

3.7 Adhesive properties of adhesives in dry/wet interfaces

To validate the efficacy of the formulations in wet interface environments, the adhesive strength of the perfusion adhesives utilizing $CaCO_3$, $CaCO_3$–SEP, $CaCO_3$–CaO, and $CaCO_3$–SEP–CaO as fillers underwent testing under both dry and wet conditions. The corresponding results are depicted in Figure 8.

The analysis of the figure reveals a substantial discrepancy solely in the dry and wet interface adhesive strength when using the calcium carbonate formulation, with the adhesive strength at the wet interface measuring only 0.85 MPa – falling short of the engineering perfusion adhesive requirement of 1 MPa. Conversely, both the $CaCO_3$–SEP and $CaCO_3$–CaO formulations demonstrated wet interface bonding strengths of 1.46 and 1.4 MPa, respectively, surpassing the required engineering perfusion adhesive bonding strength. While the adhesive strength at the wet interface remained lower than that at the dry interface, the decrease notably reduced. Because SEP can adsorb a large amount of water, and CaO can react with water, reducing the degree of wetting of the wet interface, thus reducing the impact on the adhesive strength of the infusion adhesive. Remarkably, when utilizing the $CaCO_3$–SEP–CaO composite, the adhesive strength at the wet interface achieved 1.57 MPa, aligning almost identically with the dry interface strength and displaying minimal influence from the wet interface. Hence, the application of the $CaCO_3$–SEP–CaO composite stands out as optimal for achieving superior adhesive material strength, especially in scenarios involving wet interface conditions.

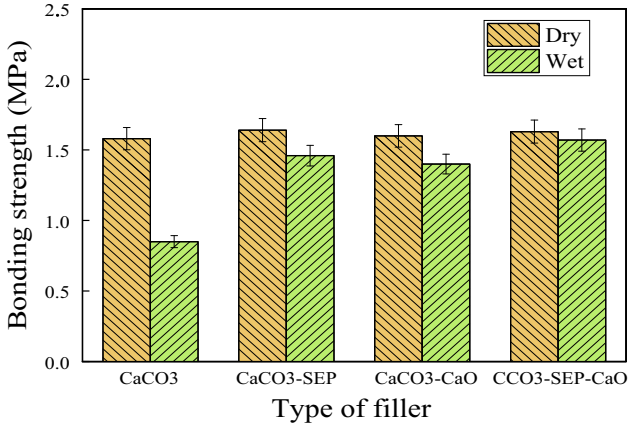

Figure 8: Bonding strength of perfusion adhesive under dry and wet conditions.

3.8 Principle of adhesive waterproofing

For a more comprehensive understanding of the moisture-proof capabilities of the perfusion adhesive, we delved into investigating its moisture-proof mechanism. The schematic diagram illustrating this mechanism is depicted in Figure 9.

Moist cement tends to generate a minute water film at the interface. When regular potting adhesives come into contact with this water film, the silane crosslinking agents within the adhesive undergo a reaction, becoming highly hydrated and subsequently initiating self-polymerization and condensation reactions to form siloxane bridges (12). This reaction leads to a substantial depletion of the silane crosslinking agent, which is detrimental to the silicone rubber's crosslinking reaction. In our research, we developed a moisture-resistant potting adhesive by blending SEP, known for its potent water-absorbing capabilities, and calcium oxide, which vigorously reacts with water,

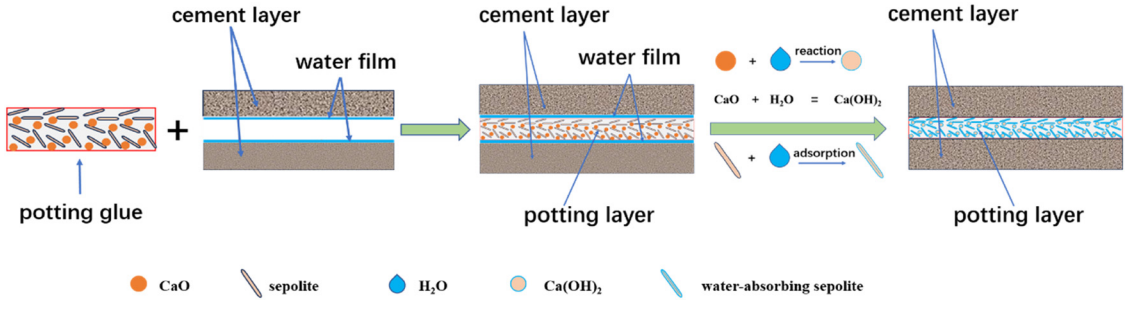

Figure 9: Schematic diagram of moisture-proof mechanism.

with silica gel to craft a single-component waterproof silicone rubber. When this moisture-resistant filling gel is injected into damp cement cracks, the surface of the SEP, rich in active hydroxyl groups, absorbs a significant amount of water (32). Simultaneously, SEP's internal tubular channels further facilitate water absorption through capillary action. Additionally, the reaction between calcium oxide and water generates calcium hydroxide, reducing the water content and preventing excessive water loss from the silica gel's crosslinking agent. Furthermore, the reaction between calcium oxide and water produces heat, further catalyzing the crosslinking reaction between the crosslinking agent and silica gel. Through the physical adsorption properties of SEP and the chemical reaction involving calcium oxide and water, the adverse impact of the water film on the silica gel's crosslinking reaction is significantly mitigated, if not completely eliminated.

4 Conclusions

In this study, a one-component silica gel potting adhesive was formulated using silane-modified SEP to enhance the adhesive's performance in moist environments. Initially, SEP underwent high-temperature calcination at 350°C to eliminate moisture content. Subsequent examination via XRD and TGA confirmed that both the crystal structure and water-absorption properties remained unaffected. Following this, various modifiers were evaluated for their effectiveness in SEP modification, with KH550 demonstrating the most optimal modification. Subsequently, the impact of KH550 dosage on adhesive performance was assessed, highlighting 2 phr as the most cost-effective dosage. Comparing the adhesive's effectiveness in wet and dry interfaces revealed that with the incorporation of SEP, the adhesive's strength remained nearly identical between wet and dry interfaces, showcasing minimal influence from the wet interface.

Author contributions: Yiyi Shi: writing – original draft, writing – review & editing; Jianqiao Liu: writing – original draft, formal analysis, and visualization; Pengyu Yang: editing and supervision; Hongzhen Wang: investigation, resources, and supervision; Shanshan Guan: investigation, methodology, and writing – review; Jiyuan Cui: investigation and data curation. All authors have read and agreed to the published version of the manuscript.

Conflict of interest: Authors state no conflict of interest.

Data availability statement: All relevant data are provided within this article.

References

(1) Li F, Yang Y, Tao M, Li X. A cement paste–tail sealant interface modified with a silane coupling agent for enhancing waterproofing performance in a concrete lining system. RSC Adv. 2019;9(13):7165–75. doi: 10.1039/C8RA10457C.

(2) Yang J, Yin ZY, Laouafa F, Hicher PY. Numerical analysis of internal erosion impact on underground structures: Application to tunnel leakage. Geomech Energy Environ. 2022;31:100378. doi: 10.1016/j.gete.2022.100378.

(3) Safan MA, Etman ZA, Konswa A. Evaluation of polyurethane resin injection for concrete leak repair. Case Stud Constr Mater. 2019;11:e00307. doi: 10.1016/j.cscm.2019.e00307.

(4) Zheng K, Yang X, Chen R, Xu L. Application of a capillary crystalline material to enhance cement grout for sealing tunnel leakage. Constr Build Mater. 2019;214:497–505. doi: 10.1016/j.conbuildmat.2019.04.095.

(5) Zhang DM, Huang ZK, Yin ZY, Ran LZ, Huang HW. Predicting the grouting effect on leakage-induced tunnels and ground response in saturated soils. Tunn Undergr Space Technol. 2017;65:76–90. doi: 10.1016/j.tust.2017.02.005.

(6) Khaloo A, Parvin Darabad Y. Investigation of mechanical properties of concrete containing liquid silicone rubber under axial loads. Shock Vib. 2021;2021:6637625. doi: 10.1155/2021/6637625.

(7) Wang K, Cheng J, Zhu Y, Wang X, Li X. Experimental research on the performance of the thermal-reflective coatings with liquid silicone rubber for pavement applications. e-Polymers. 2021;21(1):453–65. doi: 10.1515/epoly-2021-0046.

(8) Guo L, Xu H, Wu N, Yuan S, Zhou L, Wang D, et al. Molecular dynamics simulation of the effect of the thermal and mechanical properties of addition liquid silicone rubber modified by carbon nanotubes with different radii. e-Polymers. 2023;23(1):20228105. doi: 10.1515/epoly-2022-8105.

(9) Wang X, Qin Y, Zhao C. High-temperature behavior of silicone rubber composite with boron oxide/calcium silicate. e-Polymers. 2022;22(1):595–606. doi: 10.1515/epoly-2022-0051.

(10) Heng CW, Teh PL, Abdul Rahim NA, Yeoh CK. The influence of liquid silicone rubber on the properties of polyurethane elastomer/liquid silicone rubber/graphene nanoplatelets stretchable conductive materials. Prog Rubber Plast Recycl Technol. 2022;38(4):267–79. doi: 10.1177/14777606221118659.

(11) Kim J, Zollinger D, Cho W. Experimental study of the effects of moisture on the performance of concrete pavement joint sealants. Transp Res Rec. 2022;2676(7):585–96. doi: 10.1177/03611981221080136.

(12) Quang Khieu D, Dang Son BH, Thi Thanh Chau V, Dinh Du P, Hai Phong N, Thi Diem Chau N. 3-Mercaptopropyltrimethoxysilane modified diatomite: Preparation and application for voltammetric determination of lead(II) and cadmium(II). J Chem. 2017;2017:9560293. doi: 10.1155/2017/9560293.

(13) Gawenda T, Surowiak A, Krawczykowska A, Stempkowska A, Niedoba T. Analysis of the aggregate production process with different geometric properties in the light fraction separator. Materials. 2022;15:4046. doi: 10.3390/ma15124046.

(14) González JC, Molina-Sabio M, Rodríguez-Reinoso F. Sepiolite-based adsorbents as humidity controller. Appl Clay Sci. 2001;20(3):111–8. doi: 10.1016/S0169-1317(01)00062-X.

(15) Vahedi A, Rahmani M, Rahmani Z, Moghaddasi M, Talebnia Rowshan F, Kazemi A, et al. Application of polymer-sepiolite composites for adsorption of Cu(II) and Ni(II) from aqueous solution:

equilibrium and kinetic studies. e-Polymers. 2018;18(3):217–28. doi: 10.1515/epoly-2017-0170.
(16) Kaynak E, Ureyen ME, Koparal AS. Thermal characterization and flammability of polypropylene containing sepiolite-APP combinations. e-Polymers. 2017;17(4):341–8. doi: 10.1515/epoly-2016-0275.
(17) Kang F, Tu J, Zhao H, Bai Z, Zhang T. Flame retardancy and smoke suppression of silicone rubber foam with microencapsulated sepiolite and zinc borate. Polymers. 2023;15:2927. doi: 10.3390/polym15132927.
(18) Alongi J, Pošković M. Influence of nanoparticles on the morphology, thermal stability and air permeability of electrospun polylactic-acid fibres. e-Polymers. 2011;11(1):072. doi: 10.1515/epoly.2011.11.1.784.
(19) Tian L, Wang L, Wang K, Zhang Y, Liang J, Zhang Y. The sintering kinetics of shellfish porcelain reinforced by sepiolite nanofibers. R Soc Open Sci. 2018;5:180483. doi: 10.1098/rsos.180483.
(20) Pu S, Duan P, Yan C, Ren D. Influence of sepiolite addition on mechanical strength and microstructure of fly ash-metakaolin geopolymer paste. Adv Powder Technol. 2016;27(6):2470–7. doi: 10.1016/j.apt.2016.09.002.
(21) Beauger C, Laine G, Burr A, Taguet A, Otazaghine B, Rigacci A. Nafion(R)-sepiolite composite membranes for improved proton exchange membrane fuel cell performance. J Membr Sci. 2013;430:167–79. doi: 10.1016/j.memsci.2012.11.037.
(22) Zhang YD, Wang LJ, Wang F, Liang J, Ran S, Sun J. Phase transformationand morphology evolution of sepiolite fibers during thermal treatment. Appl Clay Sci. 2017;143:205–11. doi: 10.1016/j.clay.2017.03.042.
(23) Zong S, Xu X, Ran G, Liu J. Comparative study of atrazine degradation by magnetic clay activated persulfate and H2O2. RSC Adv. 2020;10(19):11410–7. doi: 10.1039/d0ra00345j.
(24) Wang F, Hao M, Liang J, Gao P, Zhu M, Fang B, et al. A facile fabrication of sepiolite mineral nanofibers with excellent adsorption performance for Cd2+ ions. RSC Adv. 2019;9(69):40184–9. doi: 10.1039/C9RA07836C.
(25) Martinez-Ramirez S, Puertas F, Varela M. Carbonation process and properties of a new lime mortar with added sepiolitel. Cem Concr Res. 1995;251:39–50. doi: 10.1016/0008-8846(94)00110-k.
(26) Tang J, Zong L, Mu B, Kang Y, Wang A. Attapulgite/carbon composites as a recyclable adsorbent for antibiotics removal. Korean J Chem Eng. 2018;35:1650–61. doi: 10.1007/s11814-018-0066-0.
(27) Wang F, Feng L, Tang Q, Liang J, Liu H, Liu H. Effect of modified sepiolite nanofibers on properties of cis-polybutadiene rubber composite nanomaterials. J Nanomater. 2013;2013:369409. doi: 10.1155/2013/369409.
(28) Giménez Pérez R, Serrano Prieto MB, San Miguel Arnanz V, Cabanelas Valcárcel JC. Recent advances in MXene/Epoxy composites: Trends and prospects. Polymers. 2022;14:1170. doi: 10.3390/polym14061170.
(29) Siddeeg SM, Tahoon MA, Alsaiari NS, Shabbir M, Rebah FB. Application of functionalized nanomaterials as effective adsorbents for the removal of heavy metals from wastewater: a review. Curr Anal Chem. 2021;17:4–22.
(30) Trelles JA, Lapponi MJ. Immobilization techniques applied to the development of biocatalysts for the synthesis of nucleoside analogue derivatives. Curr Pharm Des. 2017;23:6879–97. doi: 10.2174/1381612824666171204102204.
(31) Wang Y, Hansen CJ, Wu CC, Robinette EJ, Peterson AM. Effect of surface wettability on the interfacial adhesion of a thermosetting elastomer on glass. RSC Adv. 2021;11(49):31142–51. doi: 10.1039/D1RA05916E.
(32) Jiang X, Wang S, Ge L, Lin F, Lu Q, Wang T, et al. Development of organic–inorganic hybrid beads from sepiolite and cellulose for effective adsorption of malachite green. RSC Adv. 2017;7(62):38965–72. doi: 10.1039/C7RA06351B.